




CTAB-templated formation of CuCo₂O₄/CuO nanorods and nanosheets for high-performance supercapacitor applications

G. Sivashanmugam^{1,*} , Kunhikrishnan Lakshmi², B. Preethi³, S. Nelson⁴, and M. Sathiyaseelan⁵

¹Department of Chemistry, A.V.C. College(Autonomous), Mannampandal, Mayiladuthurai, Tamil Nadu, India

²Department of Chemistry, Anand Institute of Higher Technology, OMR Road, Chennai 603103, India

³Department of Chemistry, BS Abdur Rahman Crescent Institute of Science and Technology, Vandalur, Chennai 600048, India

⁴Department of Chemistry, T.B.M.L College, India Porayar 609307

⁵Department of Chemistry, Annai College of Arts and Science, Kovilacheri, Kumbakonam, India

Received: 8 May 2021

Accepted: 15 August 2021

Published online:

20 October 2021

© The Author(s), under exclusive licence to Springer Science+Business Media, LLC, part of Springer Nature 2021

ABSTRACT

In the present work, Copper cobaltites (CuCo₂O₄) were efficiently developed by the CTAB-assisted sonochemical process succeeded by calcination at 350 °C for 3 h. The differential scanning calorimetric analysis results showed that all the reactions ended at 300 °C. The Fourier transform infrared spectroscopy and X-ray diffraction results established the formation of spinel CuCo₂O₄/CuO. The morphological analytic results exposed that CuCo₂O₄ possesses both the nanorods and nanoparticles structure. Furthermore, cyclic voltammetry (CV) and chronopotentiometric (CP) methods were used to evaluate the electrochemical properties of various CuCo₂O₄ formed. It is observed that the freshly prepared CuCo₂O₄ electrodes exhibit a very high specific capacitance of 811 Fg⁻¹ at a scan rate of 5 mV s⁻¹ and also demonstrates superior cycling stability retaining 91% of the initial capacitance even after 3000 continuous CV cycles. Hence, typical CuCo₂O₄ could be considered as an important electrode material for supercapacitor applications.

1 Introduction

Scheming and emerging of new and effective clean energy accumulators is a significant issue in the present universal scientific research because of exhausting renewable energy resources and issues in the environment [1]. In this connection,

supercapacitors or ultracapacitors are recognized as a widespread clean energy storage device, which exhibits long cycle life, high power density, high-rate capability, fast charging/discharging, and wide range of operating temperatures [2]. Due to these significant features, supercapacitors find applications in memory backups, electric vehicle, power grids,

Address correspondence to E-mail: sivashanmugam.gss@gmail.com

hybrid-electric vehicles, etc. Ultracapacitors are classified into two types; (i) electric double-layer capacitors (EDLCs) and pseudo-capacitors. The electric double-layer capacitors store energy through ion absorption and pseudocapacitors store energy by electrochemical redox reactions [3–5]. In addition, the pseudo-capacitor materials possess higher specific capacitance than electric double-layer capacitor materials due to redox reaction [2, 6, 7].

Fascinatingly, ruthenium oxide (RuO_2) is generally acknowledged as a better alternate for pseudocapacitor electrode as it exhibits high conductivity and superior specific capacitance, and good durability. However, its high cost, toxicity, and low abundance have restricted its usage in commercial supercapacitor applications [8]. Consequently, multiple attempts have been made to prepare different transition metal oxides such as MnO_2 [9], CoO_3 [10], NiO [11], and MoO_3 [12] demonstrating outstanding electrochemical features and intensively examined as alternative materials for supercapacitor electrodes. Besides, the metal oxides, clubbed with carbon fibres were also investigated in a wide perspective [13, 14]. However, poor conductivity of these binary metal oxides regulates their employability in ultracapacitors. Furthermore, works on lithium polysulphide suspensions were focussed on as they exhibited a decrease in capacitive behaviour and caused severe damage to electrode configurations by 80% due to volume expansions during charge/discharge reactions [3–5]. Certain energy devices, direct methanol fuel cells (DMFCs) have also sought attention owing to their abundant fuel sources, low operational temperature, low environmental pollution, and high energy conversion ability [15]. Owing to the wide surface area, high electrical conductivity, outstanding electrochemical activity, higher environmental stability, and great capacitive qualities of cobalt–nickel oxides and sulphide electrodes, they are preferred for the application of high-performance SCs among the transition metal dichalcogenides and ternary transition metal oxides [16, 17].

However, recently again, mixed metal oxides have been highlighted than single metal oxides because it exhibits multiple oxidation states which may enhance good electrochemical performance [18–20]. Among the mixed metal oxides, ternary metal oxide constituents prepared from copper cobalt have fascinated much consideration owing to their high theoretical capacity, excellent redox capability, earth

abundance, corrosion resistance features in basic atmosphere, and good catalytic nature [21]. So far, various approaches have been tried on the spinel cobaltites particularly NiCo_2O_4 , which have been thoroughly examined with outstanding electrochemical properties [22–25]. A maximum specific capacitance of 1210 F/g at 2.5 A/g was revealed for the $\text{CoMoO}_4\text{@CFC}$, by Hussain et al., with an exceptional rate capability and outstanding cycling stability of 91% after 10,000 charge/discharge cycles. Though, research is being carried out, still it demands improvement in the field of supercapacitors application, so we need to examine alternative new spinel cobaltites material and discover its utilization in supercapacitors. For the abovementioned issues, CuCo_2O_4 is a best option because it exhibits good redox behaviour and high specific capacitance. When compared with single component of copper oxides and cobalt oxides, electrochemical activity and electrical conductivity of CuCo_2O_4 are reasonably higher owing to its multiple oxidation states [26]. Until now, there are a few literatures for CuCo_2O_4 as high-performance supercapacitors. For Example, Kaner and Mousavi et al. prepared mesoporous CuCo_2O_4 nanowires, which exhibit higher specific capacitance of 1210 Fg^{-1} at a current density of 2 Ag^{-1} [27]. Ryu et al. synthesized battery-like CuCo_2O_4 flowers on Ni foil, which demonstrates the specific capacitance of 692.4 Cg^{-1} at a scan rate of 5 mVs^{-1} [28]. Lou and shen et al. synthesized CuCo_2O_4 nanowires which provide the specific capacitance of 11.09 Fg^{-1} at a current of 2 mA [29]. In spite of the current development, it is still required to discover well-defined materials to further enhance their electrode properties for supercapacitor applications.

In this endeavour, we demonstrate $\text{CuCo}_2\text{O}_4/\text{CuO}$ through a CTAB-assisted sonochemical method accompanied by a calcining process. CTAB ionizes into CTA^+ and Br^- ions when it dissolves in solvents such as ethanol and water. Consequently, the CTAB ions such as CTA^+ and Br^- alter the $\text{CuCo}_2\text{O}_4/\text{CuO}$ material's morphologies. In addition, the formation of micelle or reverse micelles when it dissolves in solvents play a major role in the morphology of $\text{CuCo}_2\text{O}_4/\text{CuO}$ materials. The CTAB template acts as a growth controller, and agglomeration inhibitor for obtaining principle-oriented nanostructure. The resultant $\text{CuCo}_2\text{O}_4/\text{CuO}$ were examined by differential scanning calorimetry (DSC), Fourier transform infrared spectroscopy (FTIR), X-ray diffraction

(XRD), Energy-dispersive X-ray (EDS) spectroscopic studies, and Field emission scanning electron microscopy (FESEM) techniques. The $\text{CuCo}_2\text{O}_4/\text{CuO}$ crystal exhibits nanorods and nanoparticles structure which display a higher surface area, outstanding electron and ion transport capability, and easy approach for electrolyte transfer during electrochemical analysis. The $\text{CuCo}_2\text{O}_4/\text{CuO}$ crystal provides excellent electrochemical features with a specific capacitance of 811 Fg^{-1} at a scan rate of 5 mV s^{-1} , outstanding rate capability, and superior cyclic stability retaining 91% of the initial capacitance even after 3000 cycles at a scan rate of 100 mVs^{-1} . The excellent electrochemical features of $\text{CuCo}_2\text{O}_4/\text{CuO}$ crystal were considered as the good electrode material for supercapacitor applications.

2 Experimental

2.1 Materials

All the chemical reagents used for the experimentation work are pure. N-methyl-2-pyrrolidone (NMP), Ethanol, and Sodium hydroxide (NaOH) were purchased from SRL (India). Poly(vinylidene fluoride) (PVDF), Copper (II) nitrate trihydrate ($\text{Cu}(\text{NO}_3)_2 \cdot 3\text{H}_2\text{O}$), Cobalt (II) nitrate hexahydrate ($\text{Co}(\text{NO}_3)_2 \cdot 6\text{H}_2\text{O}$), Cetyltrimethylammonium bromide (CTAB), and carbon black were obtained from Sigma Aldrich. Furthermore, nickel foil (0.025 mm thickness) was acquired from Alfa aesar. De-ionized (DI) water was used throughout the process.

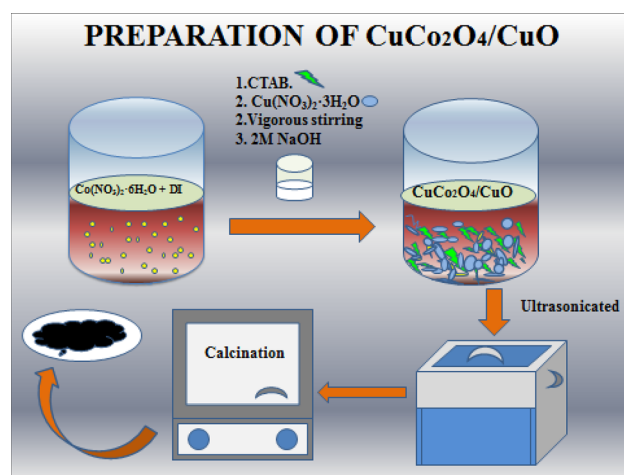
2.2 Preparation of CuCo_2O_4 crystal

$\text{CuCo}_2\text{O}_4/\text{CuO}$ were generated by using CTAB in a precipitation process and afterwards treating them with ultrasound as displayed in Scheme 1. A typical procedure is followed where, 0.90 g (0.025 M) of $\text{Cu}(\text{NO}_3)_2 \cdot 3\text{H}_2\text{O}$ and 2.183 g (0.05 M) of $\text{Co}(\text{NO}_3)_2 \cdot 6\text{H}_2\text{O}$ were dissolved in 150 ml of distilled water separately under constant stirring followed by the addition of CTAB template in cobalt nitrate hexahydrate solution carried out along with continuous stirring for half an hour. Following that, copper nitrate trihydrate was steadily applied to cobalt nitrate hexahydrate and CTAB concoction, stirring continuously for another 30 min. As the stirring progressed, a surplus of 2 M NaOH solution was

applied to the metal ion solution to complete the metal ion precipitation. Furthermore, the precipitate was ultra-sonicated in an ultrasonic cleaner (orchid scientific, model PS-500) for half an hour at room temperature. The precipitate was cleaned several times with distilled water before being filtered using Whatman filter paper. To obtain the final products, the resulting product was dried at $80 \text{ }^\circ\text{C}$ in a hot air oven and calcined at $350 \text{ }^\circ\text{C}$ for 3 h. Control synthetic methods with various CTAB concentrations were also performed for evaluation purposes. The materials namely $\text{CuCo}_2\text{O}_4\text{-A}$, $\text{CuCo}_2\text{O}_4\text{-B}$, $\text{CuCo}_2\text{O}_4\text{-C}$, and $\text{CuCo}_2\text{O}_4\text{-D}$ were prepared using 0, 0.005, 0.01, and 0.02 M of CTAB concentrations, respectively.

2.3 Material characterization

The thermal properties of the prepared $\text{CuCo}_2\text{O}_4/\text{CuO}$ were analysed using thermal analysis instrument (DSC, Hitachi- 7020 model). The phase, crystal structure, and purity of CuCo_2O_4 crystal were examined via X-ray diffraction with $\text{Cu-K}\alpha$ radiation ($1 \sim 1.5418 \text{ nm}$) by means of PANalytical X-pert PRO diffractometer instrument. A scan rate of $0.07^\circ \text{ s}^{-1}$ was used to record diffraction patterns in the 2θ range $20\text{--}80^\circ$. The internal structure and bonding properties of the prepared nanomaterials were analysed by 'Perkin-Elmer RX1' spectrophotometer with 4 cm^{-1} resolution for 20 scans. The elemental composition and surface morphologies of $\text{CuCo}_2\text{O}_4/\text{CuO}$ were studied using a thermo scientific instrument (Quattro environmental scanning electron microscopy).



Scheme 1 Preparation of $\text{CuCo}_2\text{O}_4/\text{CuO}$ Nanorods and sheets

2.4 Supercapacitor electrode preparation

The fabrication of working electrodes were done by mixing 80 wt% of $\text{CuCo}_2\text{O}_4/\text{CuO}$ with 10 wt% of acetylene black (super P) using a mortar and pestle. To this blend, 5 wt% of poly(vinylidene fluoride) (PVDF) binder was added to form a slurry. The slurry was coated on nickel foil. Then, the electrode was dried overnight at 80° C in the vacuum oven. The weight of active electrode materials was approximately 3 mg. The supercapacitor features of the developed electrodes were studied using Biologic instrument (Model SP-150). The electrochemical measurements were analysed using three-electrode cell configurations with $\text{CuCo}_2\text{O}_4/\text{CuO}$ as working electrode, platinum wire as counter electrode, and a saturated calomel electrode (SCE) as reference electrode. Moreover, 1 M KOH was used as the electrolyte. The cyclic voltammetric (CV) measurements were performed in a potential window of 0–0.5 V. The charge–discharge study was carried out at different current densities in a potential window of 0–0.4 V.

3 Results and discussion

3.1 Differential scanning calorimetric (DSC) analysis

The thermal features of the prepared $\text{CuCo}_2\text{O}_4/\text{CuO}$ nanomaterials were analysed using Differential Scanning Calorimetric (DSC) technique, shown in Fig. 1. Remarkably, there are one exothermic peak and two endothermic peaks present in the DSC curves. Prominently, there are one exothermic peak and two endothermic peaks in the present DCS curves. The loss of crystal water from the metal nitrate, evaporation of residual solvent, and loss of adsorption of water are indicated by the two endothermic peaks that appeared at 139 and 234 °C. In addition, the endothermic peak appeared at 294 °C, due to the decomposition of the precursor materials, chemical bond recombination, and lattice reconstruction to form $\text{CuCo}_2\text{O}_4/\text{CuO}$ nanomaterials. Moreover, the formations of pure CuCo_2O_4 samples are confirmed by no prominent peaks at higher temperatures. Also, 350 °C is chosen as the calcination temperature in this current endeavour.

3.2 X-ray diffraction (XRD) analysis

The XRD patterns of the freshly prepared $\text{CuCo}_2\text{O}_4/\text{CuO}$ are shown in Fig. 2. All the observed diffraction patterns obtained at 31.3, 36.9, 38.9, 45, 56, 59.5, 65.7, and 68.9° correspond to (220), (311), (222), (400), (422), (511), (440), and (531) planes coinciding with the data card (JCPDS card no. 1-1155) and could be indexed to the cubic phase (Fd3m), which affirms the development of CuCo_2O_4 . Additionally, other three diffraction peaks were observed at 35.4, 48.7, and 61.9 resembling the (– 111), (– 202), and (– 113) planes which compared with the standard JCPDS data (Card No. # 80-1268) designates the formation of copper oxide phase (Fig. 2). The present XRD results confirm the formation of $\text{CuCo}_2\text{O}_4/\text{CuO}$ multiphase crystal. Due to low thermal stability, CuCo_2O_4 forms as $\text{CuCo}_2\text{O}_4/\text{CuO}$ multiphase [30].

3.3 Fourier transform infrared spectroscopic analysis

The bonding properties of the as-synthesized $\text{CuCo}_2\text{O}_4/\text{CuO}$ were examined by FTIR spectroscopy as shown in Fig. 3a–d. The two absorption bands that appeared at 542 and 650 cm^{-1} may be the characteristic peaks and confirm the formation of CuCo_2O_4 nanomaterial. The band visible at 542 cm^{-1} is ascribed to ν_1 stretching vibration of $\text{Co}^{3+}-\text{O}^{2-}$ in the tetrahedral complexes and the band at 650 cm^{-1} may be due to ν_2 band corresponding to the $\text{Co}^{2+}-\text{O}^{2-}$ at the octahedral complexes. No variation is displayed

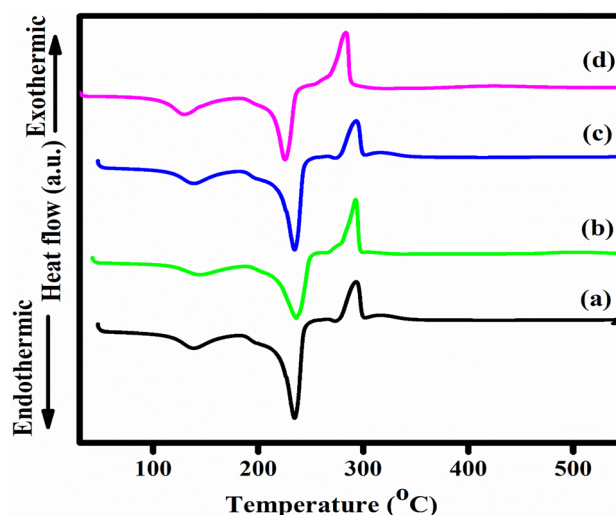


Fig. 1 DSC curves of CuCo_2O_4 samples (a) $\text{CuCo}_2\text{O}_4\text{-A}$; (b) $\text{CuCo}_2\text{O}_4\text{-B}$; (c) $\text{CuCo}_2\text{O}_4\text{-C}$; and (d) $\text{CuCo}_2\text{O}_4\text{-D}$

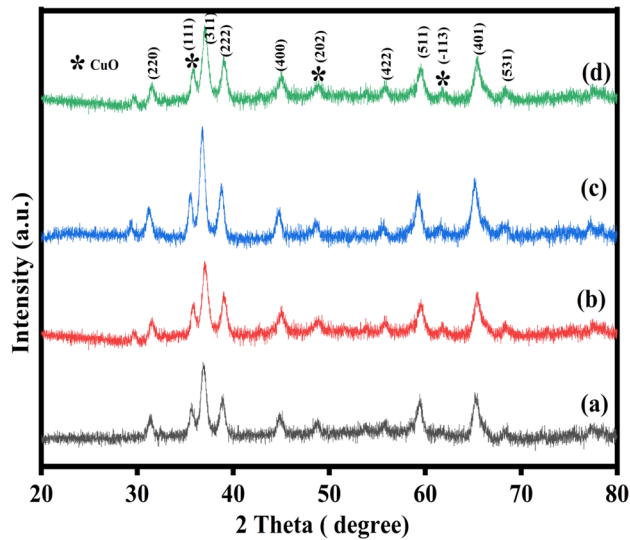


Fig. 2 XRD patterns of CuCo_2O_4 samples. (a) $\text{CuCo}_2\text{O}_4\text{-A}$; (b) $\text{CuCo}_2\text{O}_4\text{-B}$; (c) $\text{CuCo}_2\text{O}_4\text{-C}$; and (d) $\text{CuCo}_2\text{O}_4\text{-D}$

in the absorption band portrayed by the secondary phase such as CuO which can be attributed to the Co^{3+} ions and Co^{2+} occupied in tetrahedral and octahedral sites, respectively. The basic characterization results such as XRD and FTIR confirm the formation of CuCo_2O_4 [31].

3.4 Morphological analysis

The surface morphologies of $\text{CuCo}_2\text{O}_4/\text{CuO}$ nano-material were evaluated by FESEM, Energy-dispersive X-ray (EDAX) analysis and the relevant weight % values are displayed. Figure 4a and b displays the lower and higher magnification images $\text{CuCo}_2\text{O}_4\text{-A}$, which does not show any particular morphologies. $\text{CuCo}_2\text{O}_4\text{-B}$ shows the microspheres with aggregated-like morphologies and is shown in Fig. 4 c and d. Furthermore, $\text{CuCo}_2\text{O}_4\text{-C}$ (Fig. 4e, f) displays the uniform nanoparticles structure. The low and high magnification FESEM images of 3(Fig. 4g, h) disseminate both nanoparticle and nanorod structures. It is established that the size and shape are decreased when the concentration of CTAB template is increased from these results. Additionally, CTAB is more effective in the process of $\text{CuCo}_2\text{O}_4/\text{CuO}$ preparation. The energy-dispersive X-ray spectroscopic (EDAX) studies of the freshly prepared $\text{CuCo}_2\text{O}_4/\text{CuO}$ ($\text{CuCo}_2\text{O}_4\text{-D}$) is displayed in Fig. 5 and the subsequent weight % values are given in fig. The EDAX spectrum comprises different characteristic peaks such as Cu, Co, O, Al, and C confirming

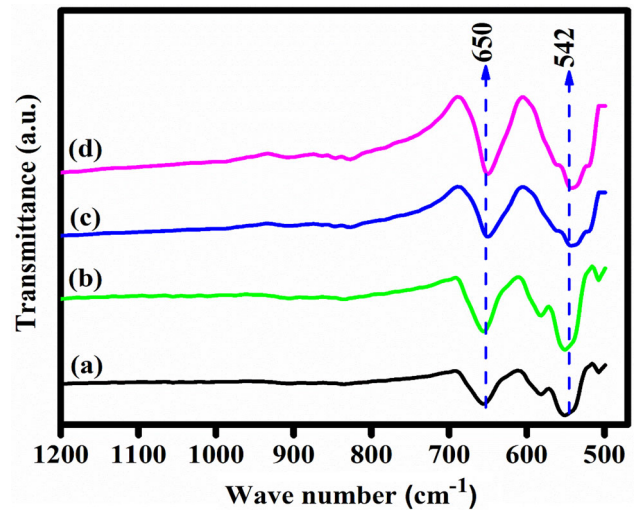
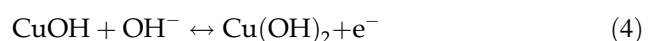
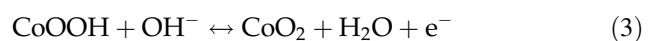


Fig. 3 FTIR spectra of CuCo_2O_4 samples (a) $\text{CuCo}_2\text{O}_4\text{-A}$; (b) $\text{CuCo}_2\text{O}_4\text{-B}$; (c) $\text{CuCo}_2\text{O}_4\text{-C}$; and (d) $\text{CuCo}_2\text{O}_4\text{-D}$

their presence in the freshly prepared $\text{CuCo}_2\text{O}_4/\text{CuO}$, while the peak C and Al accounts from the residual amount of CTAB and substrate. Therefore, XRD and EDAX analysis confirm the existence of $\text{CuCo}_2\text{O}_4/\text{CuO}$ in $\text{CuCo}_2\text{O}_4\text{-D}$ sample.

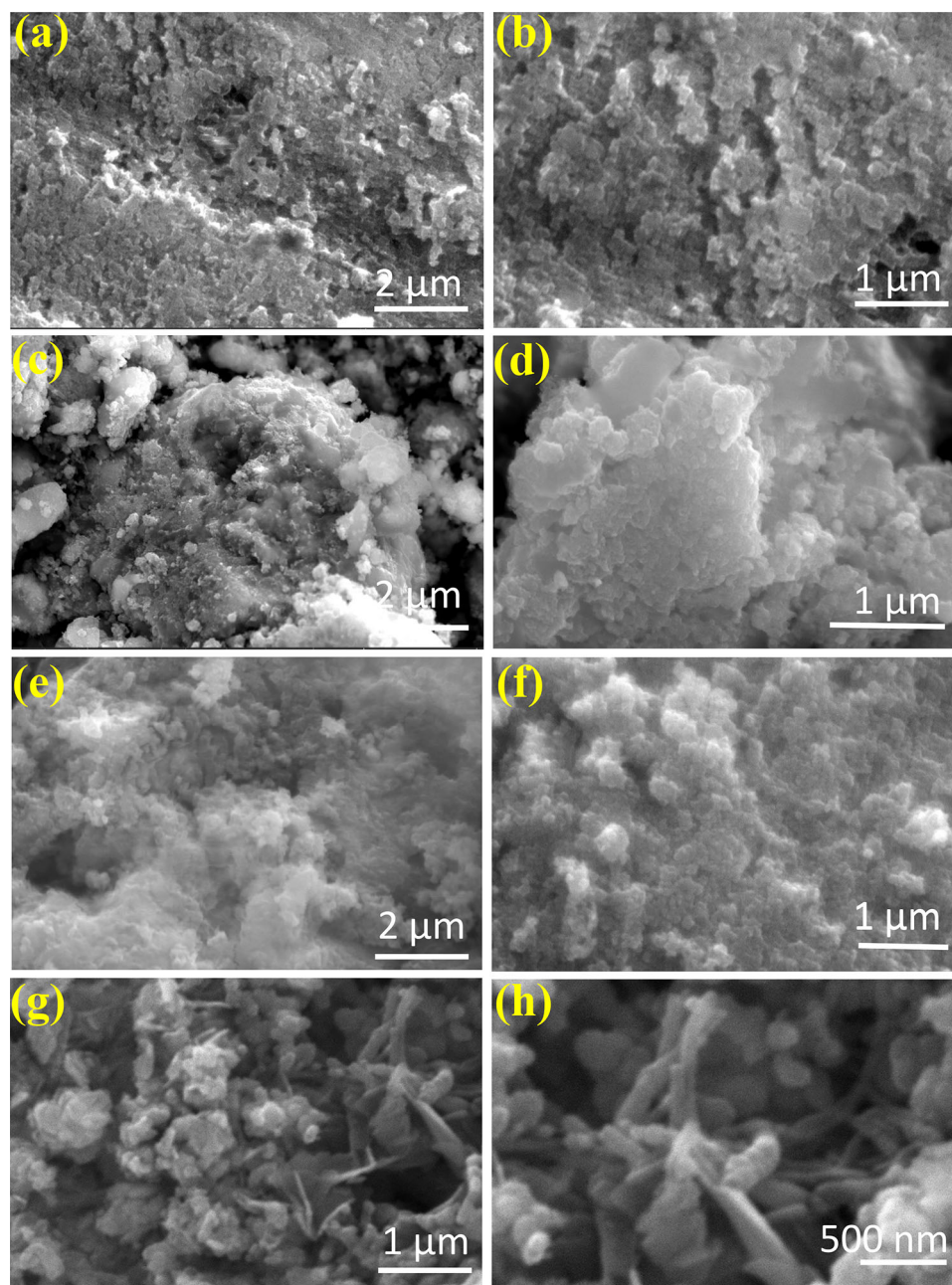
3.5 Supercapacitive performance

The supercapacitive features of the freshly prepared $\text{CuCo}_2\text{O}_4/\text{CuO}$ were investigated by cyclic voltammetry (CV) and chronopotentiometric (CP) analyses. Figure 6 (1–4) shows the CV curves of the $\text{CuCo}_2\text{O}_4/\text{CuO}$ at various scan rates. The chosen potential window for $\text{CuCo}_2\text{O}_4/\text{CuO}$ is from 0 to 0.5 V. It is noteworthy that the CV curves exhibit a pair of strong redox peaks confirming pseudocapacitive properties of the $\text{CuCo}_2\text{O}_4/\text{CuO}$ electrodes which are due to the Faradaic reaction of the Co^{4+} converted to Co^{3+} and the formation of Cu^+ from Cu^{2+} in alkaline KOH electrolyte [6]. The faradaic redox reactions can be designated as follows [21, 26]:



Furthermore, when the scan rate increases, the anodic and cathodic peak potentials shift away from each other due to the polarization and internal resistance of the $\text{CuCo}_2\text{O}_4/\text{CuO}$ electrodes. The

Fig. 4 FESEM images of CuCo_2O_4 samples: **a** & **b** CuCo_2O_4 -A; **c** & **d** CuCo_2O_4 -B; **e** & **f** CuCo_2O_4 -C; and **g** & **h** CuCo_2O_4 -D



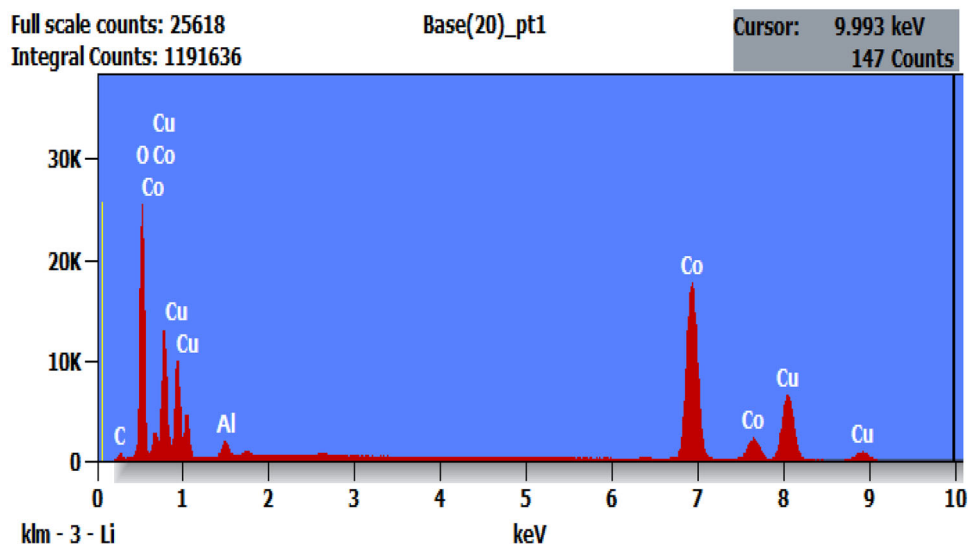
resultant CV curves are asymmetric during anodic and cathodic sweeps, designating the kinetic irreversibility of electrodes, which are due to ohmic resistance and polarization during the electrochemical Faradaic redox reaction. Interestingly, the unaltered shape of the CV curves at a higher scan rate indicates the good electrochemical stability of $\text{CuCo}_2\text{O}_4/\text{CuO}$ electrodes [3]. Figure 6e shows the CV curves of all the $\text{CuCo}_2\text{O}_4/\text{CuO}$ electrodes at a scan rate of 5 mVs^{-1} . Among all the materials, CuCo_2O_4 -D electrode provides a higher surface area,

indicating superior specific capacitance performance. Additionally from the present CV curves, the specific capacitances were determined using Eq. (5) [7, 32, 33].

$$C_{sp} = \frac{\int idV}{S \cdot \Delta V \cdot m}, \quad (5)$$

where $\int idV$ represents the integral area of CV curve, ΔV is potential window (V), m is mass of the active material (mg), and S is the scan rate (mVs^{-1}). The electrode materials such as CuCo_2O_4 -A, CuCo_2O_4 -B,

Fig. 5 Energy-dispersive X-ray (EDAX) analysis of CuCo₂O₄-D sample



CuCo₂O₄-C, and CuCo₂O₄-D provide the specific capacitances of 244, 381, 590, and 811 Fg⁻¹, respectively, at a scan rate of 5 mVs⁻¹. In addition, the calculated specific capacitance value (811 Fg⁻¹) of CuCo₂O₄-D electrode is higher than the copper, cobalt, and copper cobaltite-based crystal in earlier literatures and it may be due to the following facts: the nanorods and nanoparticles provide the high surface area for electron and ion transport. Second, the nanorods act as a conductive network between two adjacent nanoparticles and it enhance the specific capacitance. The nanosheet and nanorod morphologies provide numerous active sites which enhance faradaic redox reactions during electrochemical analysis. The nanorods shorten the conductive path length, increasing the movement of ions and electrons over the surface of electrodes [34, 35]. Figure 6f shows the rate capability of all CuCo₂O₄/CuO electrodes plotted with specific capacitance and scan rate values. It is clear that the specific capacitance values decrease when the scan rate increases from 5 to 100 mVs⁻¹, which is due to the time limiting process [27]. At lower scan rates, all the electrode materials are actively performed in the electrochemical redox reaction due to larger time which increases the capacitance. Due to short time, the outer surface electrode materials only participated in the redox reactions at higher scan rates. The CuCo₂O₄-D displays the highest specific capacitance than the other materials. Therefore, all the remaining electrochemical performance investigations such as cycling stability analysis and chronopotentiometric were carried out by using the CuCo₂O₄-D electrode.

The chronopotentiometric analyses were performed at various current densities within a potential limit from 0 to 0.4 V using aqueous 1 M KOH electrolyte solution as shown in Fig. 7. a. The CP curves show the non-linear profile confirming the pseudo-capacitive nature of the CuCo₂O₄-D electrode. Furthermore, the specific capacitance was calculated from the charge/discharge curves using Eq. (6) [36].

$$C_{sp} = \frac{I\Delta t}{m\Delta V}, \quad (6)$$

where ΔV represents potential window (V), m is mass of the active material (mg), I (A) is discharge current density, and Δt (s) is the discharge time. The specific capacitance values of CuCo₂O₄-4 are 600, 335, 160, and 120 Fg⁻¹ at various current densities of 0.5, 1, 2, and 3, respectively. The specific capacitance as a function of current density is shown in Fig. 7. The specific capacitance decreases when current densities increase, due to time limitation process, which matches with the CV results.

Capacitance retention over a long time is important for practical supercapacitor applications. Therefore, CV cycles tests up to 3000 cycles at a high scan rate of 100 mVs⁻¹ were carried to determine the cyclic stability of CuCo₂O₄-D electrodes as shown in Fig. 8. It is worth to note that the particular enhancement in the specific capacitance is detected during the first 1500 cycles, which is due to structural activation of the CuCo₂O₄-D electrodes [37, 38]. Subsequently, it is gradually decreasing and attained 91% of initial capacitance at 3000 cycles. These results reveal the outstanding cycling stability features of CuCo₂O₄.

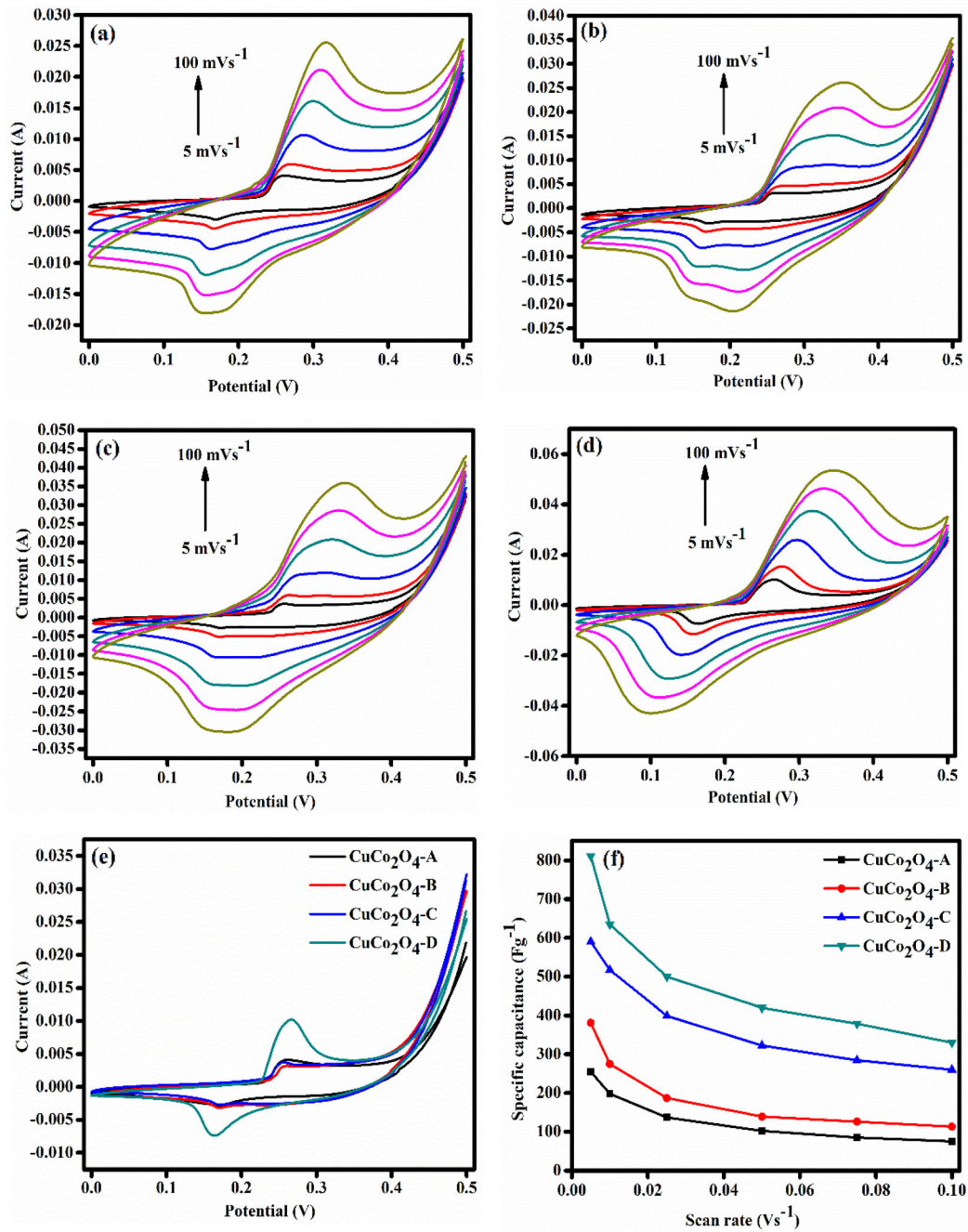


Fig. 6 CV curves of CuCo₂O₄ samples: **a** CuCo₂O₄-A; **b** CuCo₂O₄-B; **c** CuCo₂O₄-C; and **d** CuCo₂O₄-D; **e** CV curves of all CuCo₂O₄ crystals; **f** Scan rate vs Specific capacitance

These results suggest that the present CuCo₂O₄ material is a promising electrode material for supercapacitor applications.

4 Conclusion

In conclusion, a simple and low-cost CTAB-assisted sonochemical method was utilized to prepare CuCo₂O₄/CuO nanorods and sheets. The phase and internal structures of freshly prepared material were analysed using X-ray diffraction and Fourier transform infrared spectroscopic analyses. By varying the

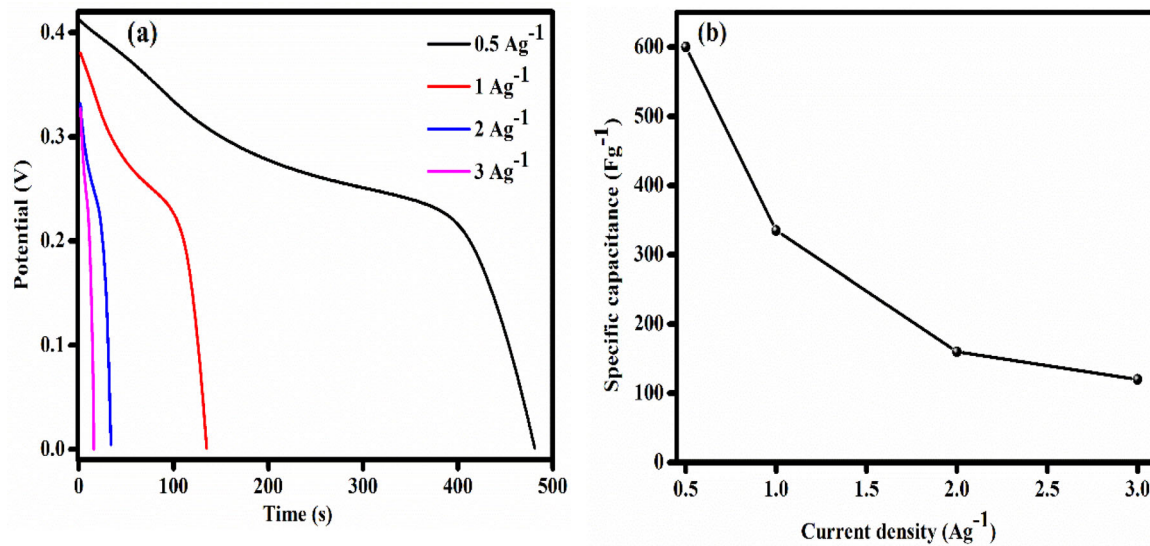


Fig. 7 **a** Chronopotentiometric (CP) Curves of CuCo₂O₄-D electrode at different current densities; **b** Current density vs Specific capacitance

concentration of CTAB template and sonochemical synthetic method, the surface morphologies can be finely altered. The FESEM analysis reveals that the prepared materials are nanorod and nanoparticle structure (CuCo₂O₄-D). It displays the highest specific capacitance of 811 at a scan rate of 5 mVs⁻¹. Interestingly, cycling stability studies of the CuCo₂O₄-D have exhibited 91% of the initial specific capacitance after 3000 cycles. The above results initiate the freshly prepared CuCo₂O₄/CuO to be

assumed as an eminent candidate for Ultracapacitor devices.

References

1. Y. Wang, H. Chai, H. Dong, J. Xu, D. Jia, W. Zhou, superior cycle stability performance of quasi-cuboidal CoV₂O₆ microstructures as electrode material for supercapacitors. *ACS Appl. Mater. Interfaces* **8**(40), 27291–27297 (2016)
2. C. Zhang, Q. Chen, H. Zhan, Supercapacitors based on reduced graphene oxide nanofibers supported Ni(OH)₂ nanoplates with enhanced electrochemical performance. *ACS Appl. Mater. Interfaces* **8**(35), 22977–22987 (2016)
3. S. Hussain, N. Ullah, Y. Zhang, A. Shaheen et al., One-step synthesis of unique catalyst Ni₉S₈@C for excellent MOR performances. *Int. J. Hydrog. Energy*. **44**, 24525–24533 (2019)
4. S. Hussain, X. Yang, M. Kashif Aslam, A. Shaheen et al., Robust TiN nanoparticles polysulfide anchor for Li–S storage and diffusion pathways using first principle calculations. *Chem Eng J* **391**, 123595 (2019)
5. S. Hussain, M.S. Javed, S. Asim, A. Shaheen, A.J. Khan et al., Novel gravel-like NiMoO₄ nanoparticles on carbon cloth for outstanding supercapacitor applications. *Ceram. Int.* **46**, 6406–6412 (2019)
6. J. Yesuraj, A.S. Samuel, E. Elaiyappillai, P.M. Johnson, V. Elumalai, M. Bhagavathiachari, A facile sonochemical assisted synthesis of α-MnMoO₄/PANI nanocomposite

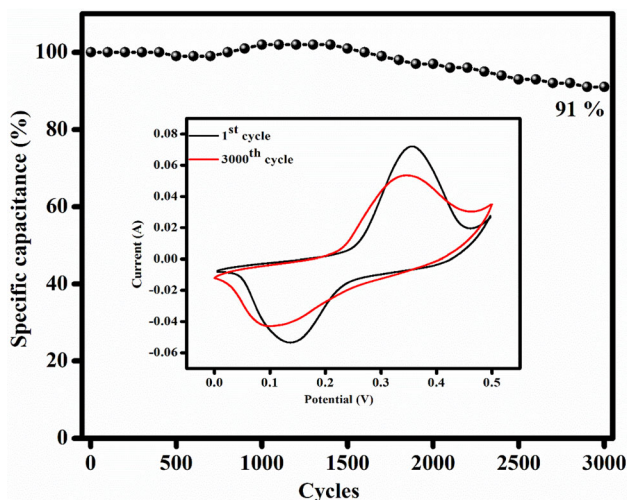


Fig. 8 Cyclic stability studies of CuCo₂O₄-D electrode at a scan rate of 100 mVs⁻¹; Inset: 1st and 3000th cycles of cyclic stability studies

- electrode for supercapacitor applications. *J. Electroanal. Chem.* **797**, 78–88 (2017)
- J. Yesuraj, S.A. Suthanthiraraj, Bio-molecule templated hydrothermal synthesis of ZnWO_4 nanomaterial for high-performance supercapacitor electrode application. *J. Mol. Struct.* **1181**, 131 (2019)
 - M. Kim, I. Oh, H. Ju, J. Kim, Introduction of Co_3O_4 into activated honeycomb-like carbon for the fabrication of high performance electrode materials for supercapacitors. *Phys. Chem. Chem. Phys.* **18**(13), 9124–9132 (2016)
 - X. Zhao et al., Prepared MnO_2 with different crystal forms as electrode materials for supercapacitors: Experimental research from hydrothermal crystallization process to electrochemical performances. *RSC Adv.* **7**(64), 40286–40294 (2017)
 - S.K. Meher, G.R. Rao, Ultralayered Co_3O_4 for high-performance supercapacitor applications. *J. Phys. Chem. C* **115**(31), 15646–15654 (2011)
 - S. Vijayakumar, S. Nagamuthu, G. Muralidharan, Supercapacitor studies on NiO nanoflakes synthesized through a microwave route. *ACS Appl. Mater. Interfaces* **5**(6), 2188 (2013)
 - M.Y. Ho, P.S. Khiew, D. Isa, W.S. Chiu, C.H. Chia, Solvothermal synthesis of molybdenum oxide on liquid-phase exfoliated graphene composite electrodes for aqueous supercapacitor application. *J. Mater. Sci. Mater. Electron.* **28**(9), 6907 (2017)
 - Y. Tiana, L. Lina, M. Ninga, S. Hussain, H. Sud et al., Novel binder-free electrode of $\text{NiCo}_2\text{O}_4@ \text{NiMn}_2\text{O}_4$ core-shell arrays modified carbon fabric for enhanced electrochemical properties. *Ceram. Int.* **45**, 16904–16910 (2019)
 - S. Bai, S. Hussain, C. Ge, M. Sufyan et al., Unique oblate-like ZnWO_4 nanostructures for electrochemical energy storage performances. *Mater. Lett.* **240**, 103–107 (2019)
 - S. Hussain, A.J. Khan, M. Arshad, M.S. Javed, A. Ahmad, S.S. Ahmad et al., Charge storage in binder-free 2D-hexagonal CoMoO_4 nanosheets as a redox active material for pseudocapacitors. *Ceram. Int.* **47**, 8659–8667 (2021)
 - S. Hussain, M. Hassan, M. Sufyan et al., Distinctive flower-like CoNi_2S_4 nanoneedle arrays (CNS– NAs) for superior supercapacitor electrode performances. *Ceram. Int.* **46**, 25942–25948 (2020)
 - Z. Xu, G. Zhao, M. Wang, J. Liang, S. Hussain, Tuning the edge-site activity of 2H phase MoSe_2 for hydrogen evolution reaction via sulfur substitution and strain engineering. *Sci. Adv. Mater.* **12**, 1–12 (2020)
 - J. Yesuraj, S. Austin Suthanthiraraj, O. Padmaraj, Synthesis, characterization and electrochemical performance of DNA-templated Bi_2MoO_6 nanoplates for supercapacitor applications. *Mater. Sci. Semicond. Process.* **90**, 225 (2019)
 - J. Yesuraj, O. Padmaraj, S.A. Suthanthiraraj, Synthesis, characterization, and improvement of supercapacitor properties of NiMoO_4 nano with polyaniline. *J. Inorg. Organomet. Polym. Mater.* (2019). <https://doi.org/10.1007/s10904-019-01189-x>
 - J. Yesuraj, E. Elanthamilan, B. Muthuraaman, S.A. Suthanthiraraj, J.P. Merlin, Bio-assisted hydrothermal synthesis and characterization of MnWO_4 nanorods for high-performance supercapacitor applications. *J. Elec. Mater.* (2019). <https://doi.org/10.1007/s11664-019-07539-2>
 - S.M. Pawar et al., Nanoporous CuCo_2O_4 nanosheets as a highly efficient bifunctional electrode for supercapacitors and water oxidation catalysis. *Appl. Surf. Sci.* **470**, 360–367 (2019)
 - Y. Lei et al., Rapid microwave-assisted green synthesis of 3D hierarchical flower-shaped NiCo_2O_4 microsphere for high-performance supercapacitor. *ACS Appl. Mater. Interfaces* **6**(3), 1773 (2014)
 - S. Khalid et al., Microwave assisted synthesis of mesoporous NiCo_2O_4 nanosheets as electrode material for advanced flexible supercapacitors. *RSC Adv.* **5**(42), 33146 (2015)
 - A.K. Yedluri, H.J. Kim, Enhanced electrochemical performance of nanoplate nickel cobaltite (NiCo_2O_4) supercapacitor applications. *RSC Adv.* **9**(2), 1115 (2019)
 - S. Xu, D. Yang, F. Zhang, J. Liu, A. Guo, F. Hou, Fabrication of NiCo_2O_4 and carbon nanotube nanocomposite films as a high-performance flexible electrode of supercapacitors. *RSC Adv.* **5**(90), 74032 (2015)
 - L. Abbasi, M. Arvand, Engineering hierarchical ultrathin CuCo_2O_4 nanosheets array on Ni foam by rapid electrodeposition method toward high-performance binder-free supercapacitors. *Appl. Surf. Sci.* **445**, 272 (2018)
 - A. Pendashteh, M.S. Rahmanifar, R.B. Kaner, M.F. Mousavi, Facile synthesis of nanostructured CuCo_2O_4 as a novel electrode material for high-rate supercapacitors. *Chem. Commun.* **50**(16), 1972–1975 (2014)
 - S. Vijayakumar, S. Nagamuthu, K.S. Ryu, CuCo_2O_4 flowers/Ni-foam architecture as a battery type positive electrode for high performance hybrid supercapacitor applications. *Electrochim. Acta* **238**, 99–106 (2017)
 - S. Gu, Z. Lou, X. Ma, G. Shen, CuCo_2O_4 nanowires grown on a Ni wire for high-performance, flexible fiber supercapacitors. *ChemElectroChem* **2**(7), 1042 (2015)
 - S. Angelov, E. Zhecheva, K. Petrov, D. Menandjiev, “The properties of a spinel copper cobaltite prepared at low temperatures and normal pressure. *Mat. Res. Bull.* **17**, 235 (1982)
 - A. Shanmugavani, R.K. Selvan, Improved electrochemical performances of $\text{CuCo}_2\text{O}_4/\text{CuO}$ nanocomposites for asymmetric supercapacitors. *Electrochim. Acta* **188**, 852 (2016)

32. A. Pendashteh et al., Highly ordered mesoporous CuCo_2O_4 nanowires, a promising solution for high-performance supercapacitors. *Chem. Mater.* **27**(11), 3919 (2015)
33. J. Yesuraj, S.A. Suthanthiraraj, DNA-mediated sonochemical synthesis and characterization of octahedron-like bismuth molybdate as an active electrode material for supercapacitors. *J. Mater. Sci. Mater. Electron.* **29**(7), 5862 (2018)
34. A.T. Aqueel Ahmed et al., Self-assembled nanostructured CuCo_2O_4 for electrochemical energy storage and the oxygen evolution reaction via morphology engineering[†]. *Small* **14**(28), 1 (2018)
35. Q. Wang, D. Chen, D. Zhang, Electrospun porous CuCo_2O_4 nanowire network electrode for asymmetric supercapacitors. *RSC Adv.* **5**(117), 96448 (2015)
36. S. Vijayakumar, S.H. Lee, K.S. Ryu, Hierarchical CuCo_2O_4 -nanobelts as a supercapacitor electrode with high areal and specific capacitance. *Electrochim. Acta* **182**, 979 (2015)
37. A.K. Das, N.H. Kim, S.H. Lee, Y. Sohn, J.H. Lee, Facile synthesis of CuCo_2O_4 composite octahedrons for high performance supercapacitor application. *Compos. Part B Eng.* **150**, 269 (2018)
38. K. Zhang, L. Lin, S. Hussain, S. Han, Core-shell $\text{NiCo}_2\text{O}_4@ZnWO_4$ nanosheets arrays electrode material deposited at carbon-cloth for flexible electrochemical supercapacitors. *J. Mater. Sci.: Mater. Electron.* **29**, 12871–12877 (2018)

Publisher's Note Springer Nature remains neutral with regard to jurisdictional claims in published maps and institutional affiliations.